

Statistical Properties of Electron Curtain Precipitation Estimated with AeroCube-6

M. Shumko^{1,2}, A.T. Johnson¹, T.P. O'Brien³, D.L. Turner⁴, A.D. Greeley²,
J.G. Sample¹, J.B. Blake³, L.W. Blum², A.J. Halford²

¹Department of Physics, Montana State University, Bozeman, Montana, USA

²NASA's Goddard Space Flight Center, Greenbelt, Maryland, USA

³Space Science Applications Laboratory, The Aerospace Corporation, El Segundo, California USA

⁴Johns Hopkins Applied Physics Laboratory, Laurel, Maryland, USA

Key Points:

- We used the dual AeroCube-6 CubeSats to identify stationary, narrow in latitude, and persistent > 30 keV precipitation in low Earth orbit. *herald curtains*
- 90% of observed curtains are narrower than 20 kilometers in latitude.
- A few curtains were continuously scattered into the atmosphere for at least six seconds.

O *second?*

15 **Abstract**

16 Curtains are a recently discovered stationary, persistent, and latitudinally narrow elec-
 17 tron precipitation phenomenon in low Earth orbit. Curtains are observed over sequen-
 18 tial passes of the dual AeroCube-6 CubeSats with their > 30 keV electron dosimeters,
 19 observed over a variety of spacecraft separations, and observed by the following space-
 20 craft for up to 65 seconds after the leading spacecraft. This study expands on the recent
 21 curtain discovery and quantifies statistical properties of 1,634 curtains observed over three
 22 years. We found that in low Earth orbit, many curtains are narrower than 10 kilome-
 23 ters in latitude and 90% are narrower than 20 kilometers. We also found that curtains
 24 are an outer radiation belt phenomena that are observed in the late morning and mid-
 25 night magnetic local times, with a higher occurrence rate at midnight. Furthermore, cur-
 26 tains are observed more often during geomagnetically active times. We tested the hy-
 27 pothesis that curtains are drifting remnants of microbursts. We found a few curtains in
 28 the bounce loss cone region in the north Atlantic Ocean, whose electrons were contin-
 29 uously scattered for at least 6 seconds as shown in one example. Therefore, curtains may
 30 be a significant source of > 30 keV electrons into the atmosphere.

31 **1 Plain Language Summary**

32 Electron curtain precipitation from space into Earth's atmosphere is a recently-discovered
 33 phenomenon observed by dual-spacecraft missions such as the AeroCube-6 CubeSats that
 34 orbit 700 kilometers above Earth's surface. Curtains appear stationary, remaining un-
 35 changed from seconds and up to a minute. Curtains are also very narrow along the satel-
 36 lite orbit (mostly in latitude). Besides these two properties, curtains and their impact
 37 on the magnetosphere and atmosphere are not well understood. Curtains are hypoth-
 38 esized to be related to another form of electron precipitation called microbursts and we
 39 tested this hypothesis. We found 1,634 curtains observed by the AeroCube-6 mission over
 40 a three year period and quantified their properties to better understand their origin. Cur-
 41 tains and microbursts share many similarities, however curtains observed in a special re-
 42 gion in the North Atlantic Ocean put this hypothesis in question. A few dozen curtains
 43 observed in this North Atlantic region were continuously precipitating into the atmosphere
 44 for multiple seconds and are unlikely to be related to microbursts. Therefore, curtains
 45 may be a significant source atmospheric ionization responsible for the natural degrega-
 46 tion of ozone.

47 **2 Introduction**

48 Curtain electron precipitation is a stationary phenomenon observed in low Earth
 49 orbit (LEO). Curtains are narrow in latitude and appear stationary for up to a minute
 50 between subsequent satellite passes. Curtains were recently discovered by Blake and O'Brien
 51 (2016) using the > 30 keV electron dosimeters onboard the dual AeroCube-6 (AC6) Cube-
 52 Sats that operated together between 2014 and 2017. This discovery was possible due to
 53 AC6's actively maintained in-track separation that varied between a few hundred me-
 54ters and a few hundred kilometers. Besides the Blake and O'Brien (2016) study, not much
 55 is known about curtains including what they are, how are they generated, their statis-
 56 tical properties, and their impact on the atmosphere. Answering these questions is an
 57 essential next step towards a more complete understanding of how curtains, and parti-
 58 cle precipitation in general, affect the magnetosphere and Earth's atmosphere.

59 In low Earth orbit, curtains are narrower than a few tens of kilometers in latitude,
 60 so a polar-orbiting LEO satellite, such as AC6, will pass through their cross-section in
 61 about a second. Therefore, in the electron count time series curtains appear sharply peaked.
 62 AC6 also observes similar-looking transient precipitation called electron microbursts. Both
 63 microbursts and curtains are peaked in the AC6 data for different reasons: microbursts
 64 primarily for being temporally short, and curtains primarily for being narrow in latitude.

need to clarify?

needs
more
explanation

Hence AC6, and other recently developed multi-spacecraft missions, are necessary to identify and distinguish between curtains and microbursts.

Since the mid 1960s, microbursts have been observed by high altitude balloons where they also appear as sharp peaks with a sub-second duration (e.g. Anderson & Milton, 1964; Brown et al., 1965; Parks, 1967). Because balloons are relatively stationary, a microburst is easily classified as a transient phenomenon. Microburst electrons have also been directly observed by LEO satellites such as The Solar Anomalous and Magnetospheric Particle Explorer (e.g. Lorentzen, Blake, et al., 2001; O'Brien et al., 2003; Douma et al., 2017). But precipitation that looks like a microburst from a single LEO satellite is ambiguous—it can be transient, stationary and narrow in latitude, or both. Thus, multi-spacecraft missions such as the Focused Investigations of Relativistic Electron Burst Intensity, Range, and Dynamics (Johnson et al., 2020 FIREBIRD-II) and AC6 (O'Brien et al., 2016) are necessary to resolve this ambiguity. While this study focuses on stationary precipitation, microbursts that were observed simultaneously by AC6 were studied in Shumko et al. (2019).

The impact of microbursts on the outer Van Allen radiation belt and Earth's atmosphere is substantial. Lorentzen, Looper, and Blake (2001), Thorne et al. (2005), Breneman et al. (2017), and Douma et al. (2019)—among others—estimated that microbursts can deplete the outer radiation belt electrons in about a day. Furthermore, Seppälä et al. (2018) modeled a 6 hour microburst storm and concluded that microbursts depleted mesospheric ozone by roughly 10%. On the other hand, the impact of curtains is unknown so it is important to understand the connection, if any, between microbursts and curtains. Curtains and microbursts can be easily misidentified from a single spacecraft so we may need to reevaluate single-satellite microburst studies. If curtains are numerous then the microburst occurrence rate and the microburst impact on the atmosphere and the outer radiation belt is overestimated.

Blake and O'Brien (2016) proposed a hypothesis that curtains are drifting remnants of microbursts. If a microburst is not completely lost in the atmosphere after the initial scatter, the remaining microburst electrons will spread out (bounce phase disperse) along the entire magnetic field line over a few bounce periods. Concurrently these electrons drift to the east, with higher energy electrons drifting at a faster rate. Therefore, if this hypothesis is true, the initially localized microburst is spread out in longitude into the shape of a curtain. The idea of curtains is not entirely new, and Lehtinen et al. (2000) predicted that energetic runaway beams driven by lightning can also create curtains.

This study expands the Blake and O'Brien (2016) study by estimating statistical properties of curtains. We use 1634 confirmed curtain observations to study the distributions of the curtain width in latitude, the geomagnetic conditions favorable to curtains, and curtain distribution in L and magnetic local time (MLT). Lastly we will address the hypothesis that curtains are drifting remnants of microbursts and show examples of curtains observed in the BLC region.

3 Instrumentation

The AC6 mission was a pair of 0.5U (10x10x5 cm) CubeSats built by The Aerospace Corporation and designed to measure the electron and proton environment in low Earth orbit (O'Brien et al., 2016). AC6 was launched on 19 June 2014 into a 620x700 km, 98° inclination orbit. The AC6 orbit over the three year mission lifetime was roughly dawn-dusk, and precessed only a few hours in MLT; 8-12 MLT in dawn and 20-24 MLT in dusk. The two AC6 spacecraft, designated as AC6-A and AC6-B, separated after launch and were in proximity for the duration of the three-year mission—maintained by an active attitude control system. The attitude control system allowed them to precisely control the amount of atmospheric drag experienced by each AC6 unit using the surface area

other more background disc. of
other precip. events? microbursts here
(e.g. -
)

Blake '96

single vs
spont.

crew / space...

ok but few work

✓
examining
curtain
width
duration
...

SIC

of their solar panel “wings”. By changing their orientation, AC6 was able to maintain a separation between 2–800 km, confirmed by the Global Positioning System. The two AC6 units were in a string of pearls configuration, so one unit, typically unit A, was leading the other by an in-track lag: the time it would take the following spacecraft to catch up to the position of the leading spacecraft. To convert between the AC6 in-track separation and in-track lag, the AC6 orbital velocity was used. AC6’s orbital velocity was 7.6 km/s and varied by as much as 0.1 km/s. The in-track lag was readily available with the Global Positioning System, which makes it easy to study precipitation phenomena observed at the same time, and at the same position by shifting one time series by the in-track lag.

Each AC6 unit contains three Aerospace microdosimeters (licensed to Teledyne Microelectronics, Inc) that measure the electron and proton dose in orbit (O’Brien et al., 2016). The dosimeter used for this study is dos1 with a > 30 keV electron threshold. ~~dos1 is used for this study because the other dosimeters either responded primarily to protons or were not identical between unit A and B. All dosimeters sample at 1 Hz in survey mode, and 10 Hz in burst mode. 10 Hz data was readily available from both AC6 units from June 2014 to May 2017 while their in-track lag was less than 65 seconds, and at times was a fraction of a second.~~ Figure A1 shows the distribution of 10 Hz data as a function of AC6 in-track lag. The variety of AC6 separations and data availability over the three-year mission makes it possible to study transient electron microburst precipitation (Shumko et al., 2019) and now stationary electron curtain precipitation.

4 Methodology

4.1 Curtain Identification

The 10 Hz data was used to identify curtains with two criteria that are described below: a high spatial correlation, and prominently peaked. Before we applied the identification criteria, the AC6-B time series was shifted by the in-track lag to spatially align it with the AC6-A time series.

The first identification criterion is a 1-second rolling Pearson correlation applied to both time series. Spatial features with a correlation greater than 0.8 are considered highly correlated. The second criterion is applied to any features that are highly correlated, to check if they are also prominently peaked. To find peaked precipitation, we used a method similar to the method used by Blum et al. (2015) to identify precipitation bands and by Greeley et al. (2019) to identify microbursts. Our method quantified the number of Poisson standard deviations, σ , that a dos1 count rate is above a 10-second centered running average, B_{10} . Locations where dos1 is at least two σ above B_{10} , in other words $dos1 > 2\sqrt{B_{10}} + B_{10}$, are considered prominently peaked.

We tuned the detection parameters to identify many candidate curtains while being feasible to check every detection. One author visually inspected 6,149 candidate curtains and 1,634 quality curtains were confirmed. Four curtain examples are shown in Fig. 1. In each example, the unmodified time series is shown in the top row and the spatially-aligned time series the bottom row. The in-track lag used to shift the bottom row is annotated by dt , corresponding to an AC6 in-track separation annotated by s . The bottom row shows highly correlated curtains observed at the same location for at least 3 to 26 seconds.

4.2 Differentiating Between Drifting and Precipitating Curtains

The AC6 dosimeters lack the necessary pitch angle resolution to differentiate between drifting and precipitating electrons to test the Blake and O’Brien (2016) hypothesis that curtains are the drifting remnants of microbursts. Fortunately, one common method

CC vs dt?

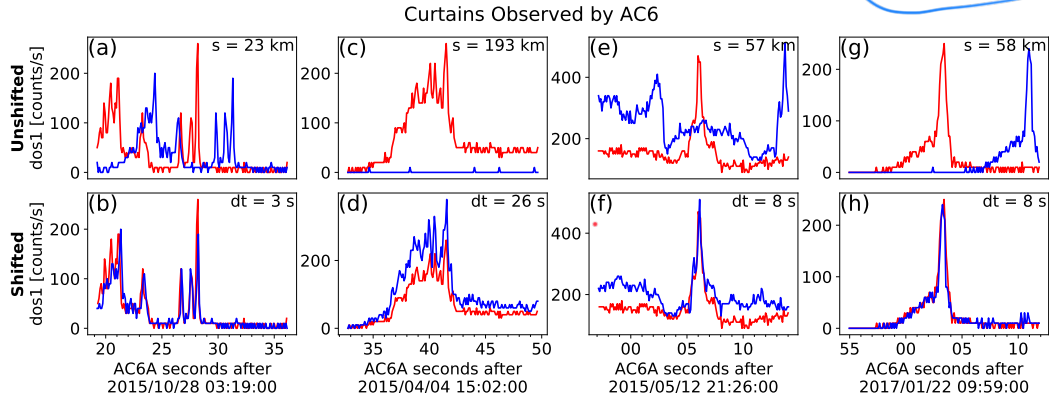


Figure 1. Four examples showing the > 30 keV electron time series data taken by AC6 at the same time (unshifted) in the top row and at the same position (shifted by dt seconds) in the bottom row. AC6-A, whose data is shown with red curves, was s kilometers ahead of AC6-B. To show the data at the same position the AC6-B time series was shifted by the in-track lag annotated by dt . These examples show that curtain precipitation was highly correlated for up to 26 seconds.

of distinguishing between precipitating, drifting, and trapped particles is using particle measurements in conjunction with the location of the South Atlantic Anomaly (SAA).

Earth's magnetic field is asymmetric, which creates a region of weaker magnetic field in the South Atlantic Ocean called the South Atlantic Anomaly. The weaker magnetic field in the SAA naturally differentiates particles by pitch angle into trapped and quasi-trapped populations. While some particles observed in LEO are trapped and will execute closed drift paths, most particles observed in LEO are quasi-trapped: they drift around the Earth until they reach the SAA. Within the SAA, the weaker magnetic field strength can lower the particle's mirror point altitude into the atmosphere, where collisions with the atmospheric ions are more numerous and the particle is lost.

Particles that are quasi-trapped have pitch angles in the drift loss cone and will precipitate within one drift period (often within the SAA). Particles with smaller equatorial pitch angles (less than $\approx 6^\circ$) that are lost in the atmosphere within one bounce are in the bounce loss cone (BLC). Traditionally, we define a BLC particle if its mirror point altitude is at or below 100 km in either hemisphere.

In most regions outside of the SAA and its conjugate point in the North Atlantic, AC6 will observe a combination of drift and bounce loss cone electrons. In the SAA, AC6 does not only observe electrons that are immediately lost, but a combination of electrons that are in the drift loss cone, bounce loss cone, and trapped (a trapped electron that locally mirrors at AC6's altitude in SAA will mirror at higher altitudes everywhere else). In the region magnetically conjugate to the SAA in the North Atlantic, AC6 only observes electrons in the BLC. Here, if an electron makes it to AC6's altitude, it might be in the local loss cone and precipitate in the local hemisphere. Alternatively, the electron can mirror at or below AC6 and bounce to its conjugate mirror point deep in the atmosphere or below sea level in the SAA. Therefore, any electrons observed in the BLC region must rapidly precipitate. (\rightarrow in 1 bounce - \times sec for 30 keV e-)

We estimated the BLC region for locally-mirroring electrons in the North Atlantic Ocean using the IRBEM-Lib magnetic field library and the Olson-Pfizer magnetic field model (Boscher et al., 2012; Olson & Pfizer, 1982). We defined a latitude-longitude grid, with a $\approx 0.5^\circ \times 0.5^\circ$ grid size, spanning the North Atlantic at 700 kilometer altitude

(a typical altitude for AC6), and estimated the local magnetic field strength. For each latitude-longitude point we traced the magnetic field line to the southern hemisphere and found the conjugate mirror point altitude. If the conjugate mirror point is at or below 100 kilometers, the electron is likely lost and the associated grid point is considered to be in the BLC. Furthermore, a more rigorous bounce loss cone criterion is the conjugate mirror point altitude below sea level. In this case, the electron is definitely lost. Since AC6 can measure locally-mirroring electrons in the North Atlantic, the spacecraft altitude determines the upper bound conjugate mirror point altitude in the SAA. The BLC region estimated by this method closely matches the BLC region shown in Comess et al. (2013, Figure 1) and Dietrich et al. (2010, Figure 3). Furthermore, we repeated the same analysis using the Tsyganenko 1989 model (Tsyganenko, 1989), which yielded similar boundaries.

5 Results

address

In this study we *answered* three questions:

1. What is the distribution of curtain widths in latitude?
2. When and where are curtains observed?
3. Are curtains drifting or locally precipitating?

We then compared some of these results to the > 30 keV microburst distribution from Shumko et al. (2019).

5.1 Curtain Width

We quantified the curtain width in the dos1 time series as the width at half of the curtain's topographic prominence: the height of the peak above the lowest contour that encircles the peak but contains no higher peak. The spatial width of a curtain is then the product of the observed width in time and AC6's orbital velocity. The curtain width is measured along AC6's orbit track which is mostly in latitude, therefore the estimated curtain widths are also mostly in latitude. The distribution of curtain widths is shown in Fig. 2 by the thick black curve. Curtains are very narrow. Many curtains are narrower than 10 km in latitude, and 90% are narrower than 20 km in latitude.

We then compared the curtain width distribution to the microburst size distribution estimated in Shumko et al. (2019). Shumko et al. (2019) estimated the microburst size distribution with microbursts that were observed simultaneously by both AC6 units. Thus, the microburst size must be larger than the AC6 separation. The red curve in Fig. 2 shows the microburst distribution estimated as the ratio of the number of simultaneous microbursts to all microbursts observed in each separation bin.

5.2 When and Where Are Curtains Observed

The distribution of curtains in L and MLT is shown in Fig. 3. Figure 3a shows the distribution of the observed curtains while Fig. 3b shows the same distribution normalized by the number of quality 10 Hz samples that AC6 took at the same location in each L-MLT bin. This normalization is shown in Fig. 3c. The normalized curtain distribution in Fig. 3b shows an enhanced curtain occurrence in the outer radiation belt in late morning and midnight MLT regions.

We also *quantified* the geomagnetic conditions favorable for curtains. Figure 4a shows the distribution of the minute cadence Auroral Electrojet (AE) index between 2014 and 2017 in solid black. Furthermore, the distribution of the AE index when curtains were observed is shown by the solid blue lines, and when microbursts were observed by the

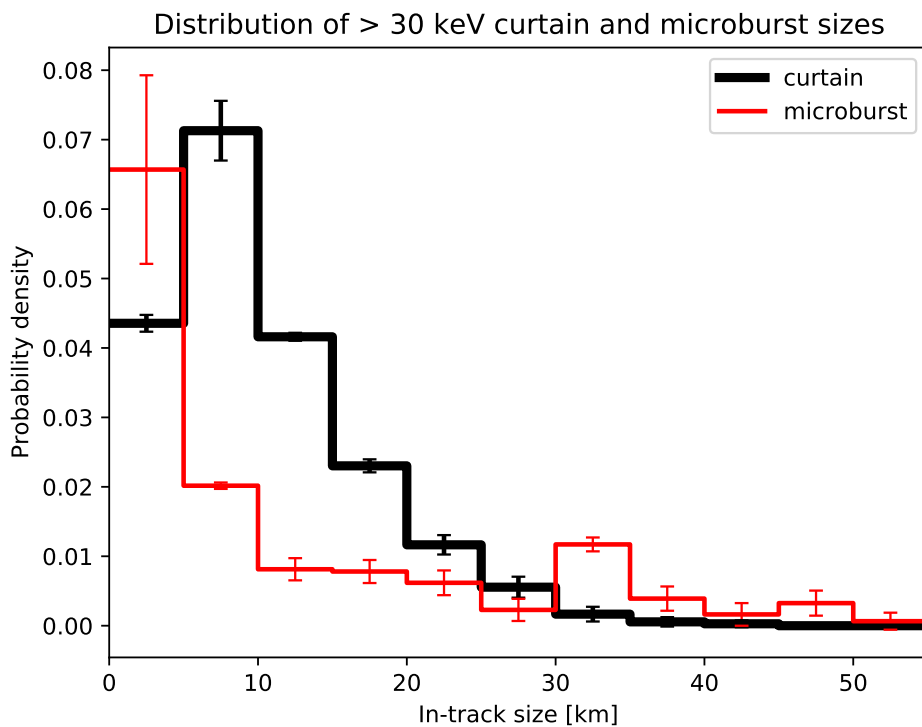


Figure 2. The distribution of curtain width in latitude is shown by the thick black lines, and the distribution of microburst sizes is shown by the red lines for microbursts that were simultaneously observed by AC6. The microburst distribution is adapted from Shumko et al. (2019). The error bars are the Poisson standard error.

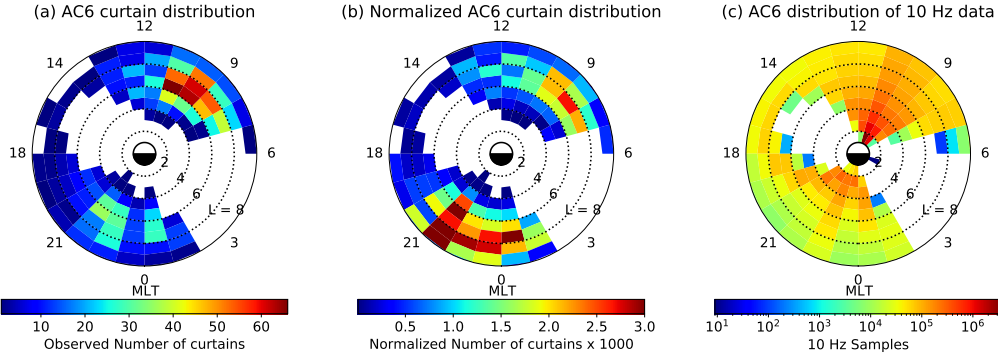


Figure 3. The distribution of observed curtains by L shell and MLT. Panel a shows the locations of all observed curtains used in this study. Panel b shows the curtain distribution normalized by the number of quality 10 Hz samples taken in each bin, shown in panel c. The white bins in panels a and b show where no curtains were observed. In panel c the white bins show where AC6 did not take any 10 Hz data at the same location.

dashed green lines. Both microbursts and curtains are observed during active geomagnetic times, but curtains are also observed relatively more often at low geomagnetic activity. Lastly, we normalized the microburst and curtain distributions in Fig. 4a ~~assuming an unrealistic, but insightful, scenario where any AE index is equally probable~~. The normalized distributions are shown in Fig. 4b and they emphasize that both curtains and microbursts occurrence frequency increases with [↑]AE index. ✓

5.3 Local Atmospheric Precipitation

Figure 5a shows a map of the northern BLC region in the North Atlantic. The solid blue line is the northern boundary where an electron that mirrors locally at 700 km has a conjugate mirror point at 100 km in the SAA. Immediately south of the solid blue line, the conjugate mirror altitude rapidly decreases towards, and below, sea level. The dashed blue line is the boundary where the conjugate mirror point altitude is at sea level. South of this line the ~~mirror point~~ ^(red) mirror point is inside the Earth. For reference, AC6 takes about 30 seconds to move between the solid and dashed blue curves. The two dotted black curves in Fig. 5a are roughly the boundary of the outer radiation belt, defined as $L = 4 - 8$. ✓

We found 36 curtains that were observed inside the BLC region. Figure 5b-e shows 4 curtain examples (AC6-B time shifted by the in-track lag), along with the AC6 in-track lag, L and MLT during the observations annotated. The AC6 locations where these curtains were observed are shown in Fig. 5a with the red stars and the corresponding panel labels. ✓

6 Discussion

6.1 Curtain Width

Curtains are ~~very~~ ^{at} narrow in latitude. Figure 2 shows that the width of most curtains is on the order of 10 kilometers and 90% are narrower than 20 km. Scaled to the magnetic equator, ~~where we presume curtains are generated~~, these widths correspond to a source with a radial scale size of a few hundred kilometers. As shown in Fig. 1, it is remarkable that some curtains remain stationary and maintain a fine structure after multiple seconds with little observable difference. However, some curtains appear to be

(1-14 sec?)
as obs. by
GO s/c

Distributions of the Auroral Electrojet index for curtains and microbursts

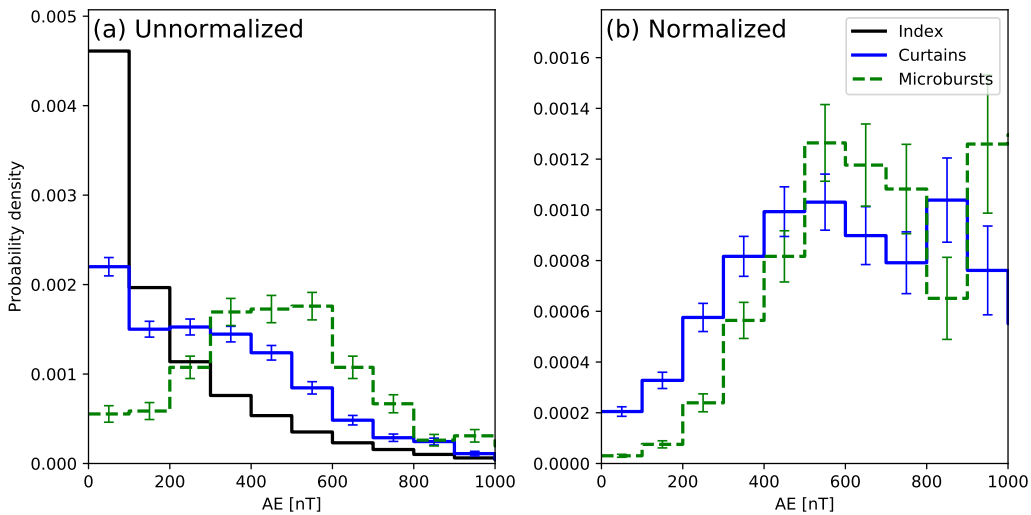


Figure 4. Panel a shows the distribution of the Auroral Electrojet (AE) index when curtains and microbursts were observed, shown by the solid blue and dashed green lines, respectively. For reference the distribution of the AE index between 2014 and 2017 is shown by the black lines. The AE distribution for microbursts is adapted from Shumko et al. (2019) and the error bars represent the Poisson standard error. Panel b shows the curtain and microburst distributions, that are normalized by the AE index, and represent the distributions assuming that any AE index is equally probable.

266 slightly and systematically shifted in latitude, while maintaining their fine structure (not
267 shown).

268 If curtains are remnants of microbursts, then the distribution of curtain widths in
269 latitude should correspond to the microburst size distribution. Figure 2 shows a good
270 correspondence between the distribution of curtain widths in latitude and the microburst
271 size distribution from Shumko et al. (2019). Therefore, it is reasonable to believe that
272 curtains and microbursts are related, but this result needs to be closely inspected for sources
273 of bias.

274 The microburst scale size distribution, as described in Shumko et al. (2019), is the
275 fraction of microbursts observed simultaneously to all microbursts observed either sim-
276 ultaneously or by only one AC6 unit. A microburst observed simultaneously must be larger
277 than the spacecraft separation so the microburst distribution is a lower bound. Further-
278 more, the detection algorithm described in section 4.1 loses sensitivity for wider curtains.
279 For curtains with a width similar to the detection algorithms 10-second baseline, the base-
280 line will be elevated making the curtain peak less pronounced. The result of this bias
281 is similar to the bias inherent in the microburst distribution—both distributions are un-
282 derestimated. These biases are difficult to quantify, but we believe that they likely too
283 small to qualitatively change the interpretation that microburst and curtain size distri-
284 butions are similar.

-9-
doesn't seem to be here
supports this

* since dists show
↑ before sensitivity
limit it may be
OK??

✓

are there in
induced stat?

X

14 mention
sooner

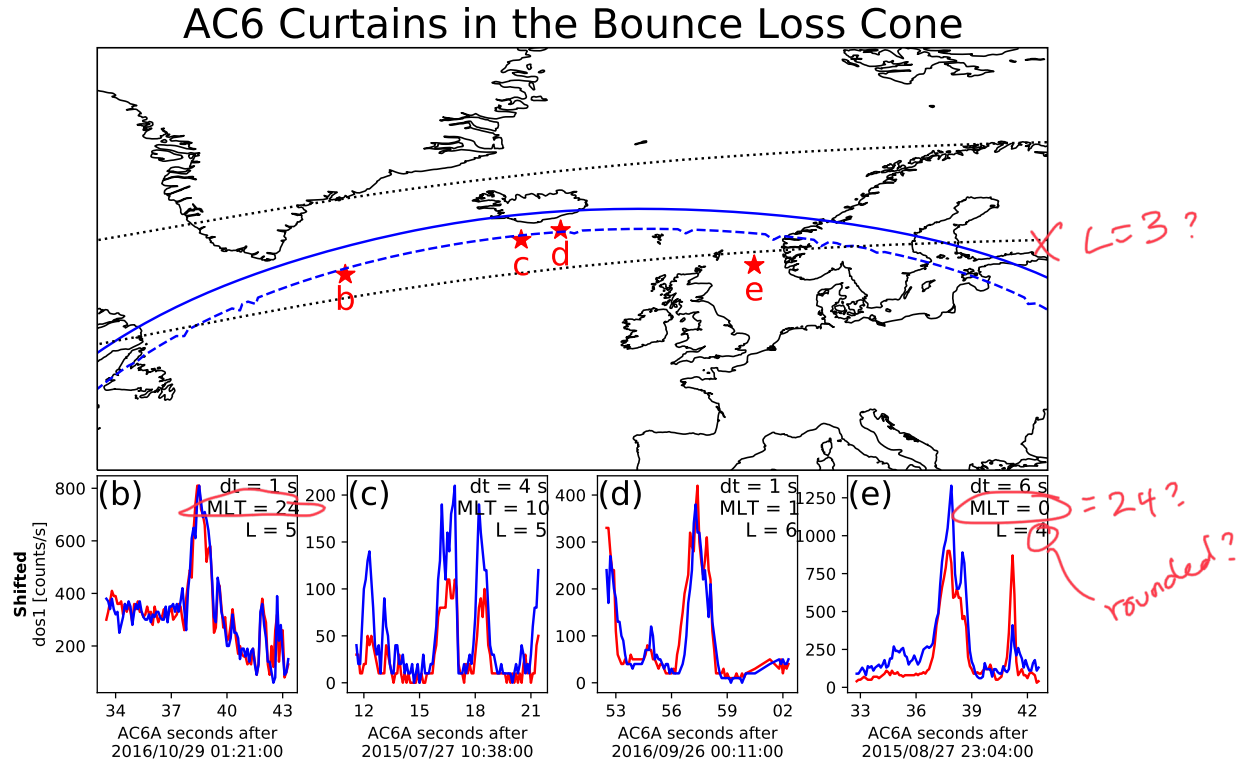


Figure 5. Curtains observed in the bounce loss cone region. Panel a shows a map of the North Atlantic region with the outer radiation belt, defined by $L = 8$, shown with the dotted black curves. The solid blue curve shows the northern boundary of the bounce loss cone region. Along this curve, electrons locally mirroring at 700 kilometers altitude have a conjugate mirror point at 100 kilometers altitude in the SAA. A more strict bounce loss cone criterion is the dashed blue curve that represents a conjugate mirror point altitude at sea level in the SAA. The 4 red stars with labels show the locations of the curtain examples shown in the corresponding panels b-e. The panels b-e show the 4 example curtains with the AC6-A data shown by the red line and the time-shifted AC6-B data with the blue line. AC6-A was ahead in all examples except panel d.

Imhotep 186

Nakamura?

285 6.2 When and Where Are Curtains Observed

286 Figure 3b shows that curtains likely originate in the outer radiation belt and are
 287 observed relatively more in the late evening than late morning regions. Unfortunately,
 288 the limited AC6 coverage prevents a complete curtain distribution in MLT. This distribution,
 289 though limited, appears to be similar to the L-MLT distribution of microbursts
 290 from prior studies (e.g. O'Brien et al., 2003; Douma et al., 2017). The MLT region with
 291 the most frequently observed curtains and microbursts are opposite: microbursts are pre-
 292 ferentially observed in the late morning, while curtains are mainly observed near midnight.
 293 The statistics at high L are rather limited because AC6 rapidly crosses high L shells. Nev-
 294 ertheless, Fig. 3b hints that curtains near midnight MLT were observed to L shells pos-
 295 sibly outside the outer radiation belt.

296 Figure 4 shows that the microburst and curtain observations are both associated
 297 with an enhanced AE, although curtains show a slight preference to lower AE index. As-
 298 suming the Blake and O'Brien (2016) hypothesis, one possible explanation is that dur-
 299 ing quiet conditions, the remnant microburst electrons are more likely to drift undisturbed
 300 and AC6 is more likely to observe the fine, highly-correlated curtain structure. In con-
 301 trast, during active conditions, the curtain electrons are still drifting, but the dynam-
 302 ics of an actively-changing magnetosphere can easily perturb curtain electrons until AC6
 303 no longer observes a highly correlated structure at the same location.

304 6.3 Curtains Observed in The Bounce Loss Cone

305 The evidence presented so far hint at, but not directly confirm, that curtains are
 306 connected to microbursts. But the few curtains that were observed in the bounce loss
 307 cone and shown in Fig. 5 put the hypothesis into question. These curtains were observed
 308 near the sea level mirror altitude curve, thus they were not drifting and were precipitat-
 309 ing for as long as 6 seconds, as shown in Fig. 5e. The curtain precipitation persisted for
 310 multiple bounce periods (≈ 1.5 seconds for 30 keV electrons in this region). This is a
 311 surprising result because there are relatively few mechanisms capable of persistently scat-
 312 tering electrons. This mechanism must be radially localized near the magnetic equator
 313 on a scale of a few hundred kilometers. One candidate mechanism is a direct current elec-
 314 tric field that is parallel to the background magnetic field that lowers the electron mir-
 315 ror point to AC6 altitudes. To find the minimum potential we assume the electron is barely
 316 trapped and has a 100 kilometer conjugate mirror point altitude in the SAA, so initially
 317 the electron will mirror above AC6 in the bounce loss cone region.

318 To find the parallel potential, $q\Phi$, we use the kinetic energy, W , of a 30 keV elec-
 319 tron at its initial mirror point with a magnetic field strength of B_i . The kinetic energy
 320 at the initial mirror point can be written as $W_i = \mu B_i$ where μ is the first adiabatic
 321 invariant that is conserved during this acceleration. When a parallel potential acts on
 322 the electron of charge q and does $q\Phi$ amount of work the electron will mirror closer to
 323 Earth's surface and mirror at a field strength B_f where its final energy is $W_f = \mu B_f$.
 324 Now we relate the initial and final kinetic energy of the electron,

$$\mu B_f = \mu B_i + q\Phi. \quad (1)$$

325 Then we solve for $q\Phi$ and substitute μ to express the above equation as a function of the
 326 initial kinetic energy

$$q\Phi = W_i \frac{(B_f - B_i)}{B_i}. \quad (2)$$

327 The parallel potential is proportional to W_i so a larger potential is necessary to accel-
 328 erate higher energy electrons. AC6 dos1 electron energy response increases rapidly from
 329 30 keV to a peak at 100 keV (O'Brien et al., 2019, Figure 2), therefore our assumption

how do properties of
BLC curtains compare
+ others, e.g. SPC, Δt,
etc.

330 that $W_i = 30$ keV will underestimate the parallel potential. In reality, the counts ob-
 331 served by AC6 is a convolution of, among other things, the AC6 dos1 electron energy
 332 response and the falling electron energy spectrum. Thus, the majority of electrons that
 333 AC6 observed have energies close to 30 keV and the $W_i = 30$ is an appropriate approx-
 334 imation.

335 We again used IRBEM-Lib to estimate $q\Phi$. For each example curtain in Fig. 5, we
 336 first estimated the local magnetic field, B_f , that the electron descended to after the ac-
 337 celeration. Then we traced the local field line into the SAA. We estimated B_i at 100 kilo-
 338 meters altitude in the SAA for barely trapped electrons. With the initial and final B ,
 339 along with $W = 30$ keV, the minimum potential was between $q\Phi = 1 - 4$ kV for the
 340 4 examples shown in Fig. 5.

341 The range of estimated potentials is typical for the aurora. Partamies et al. (2008)
 342 used the observations made by the Fast Auroral SnapshoT (FAST) mission and reported
 343 that the auroral inverted-V electron precipitation structures, with electron energies up
 344 to a few tens of keV, were accelerated by 2-4 kV parallel potentials. The inverted-V struc-
 345 ture and curtains share a number of similarities including: their energy, latitudinal width,
 346 and high occurrence rate in the midnight MLT region. A possible connection between the
 347 inverted-V structures is intriguing, but by itself AC6 can not easily test this hypothe-
 348 sis. A follow-on study can incorporate the list of observed curtains with ground-based
 349 auroral imagers and look for simultaneous occurrence of curtains and meso-scale auro-
 350 ral arcs.

351 Outside of the BLC, the lack of pitch angle information makes the AC6 electron
 352 data ambiguous, but the curtains observed in the BLC suggest that some curtains con-
 353 tinuously precipitate for multiple seconds. Curtains could be a significant source of en-
 354 ergetic electrons into the atmosphere. Energetic electron precipitation produces odd Ni-
 355 trogen (HO_x) that is currently underestimated by atmospheric models such as the widely-
 356 used Whole Atmosphere Community Climate Model (WACCM) (e.g. Randall et al., 2015).
 357 A comprehensive study of the curtain impact on the atmosphere can be done with an
 358 AC6-like mission with pitch angle and energy resolution.

359 7 Conclusions

360 The 1,634 confirmed curtains allowed us to make the following inferences:

- 361 Curtains are very narrow—90% are less than 20 kilometers wide in latitude.
- 362 Curtains are observed in the outer radiation belt, predominately in the midnight
- 363 and the late morning MLT regions, and during active geomagnetic periods.
- 364 Some curtains continuously precipitate into the atmosphere for multiple seconds.

365 Curtain precipitation is remarkably narrow with a fine structure that persists for
 366 multiple seconds. Either the scattering mechanism that continuously generates curtains
 367 is physically static for multiple seconds, or the curtain electron drift is often undisturbed.

368 The curtain-microburst relationship hypothesized in Blake and O'Brien (2016) is
 369 not clear. The two results in support of the hypothesis are: curtain width and microburst
 370 size distributions are very similar, and the limited AC6 coverage in MLT shows that both
 371 occur in similar locations in the magnetosphere. But curtains observed in the bounce
 372 loss cone complicate this interpretation. Some curtains continuously precipitate for at
 373 least a few seconds, and can be a significant source of energetic electron precipitation
 374 into the atmosphere. Lastly, we found that the continuous scattering of curtain electrons
 375 can be explained by a parallel direct current electric field, possibly relating curtains to
 376 the aurora.

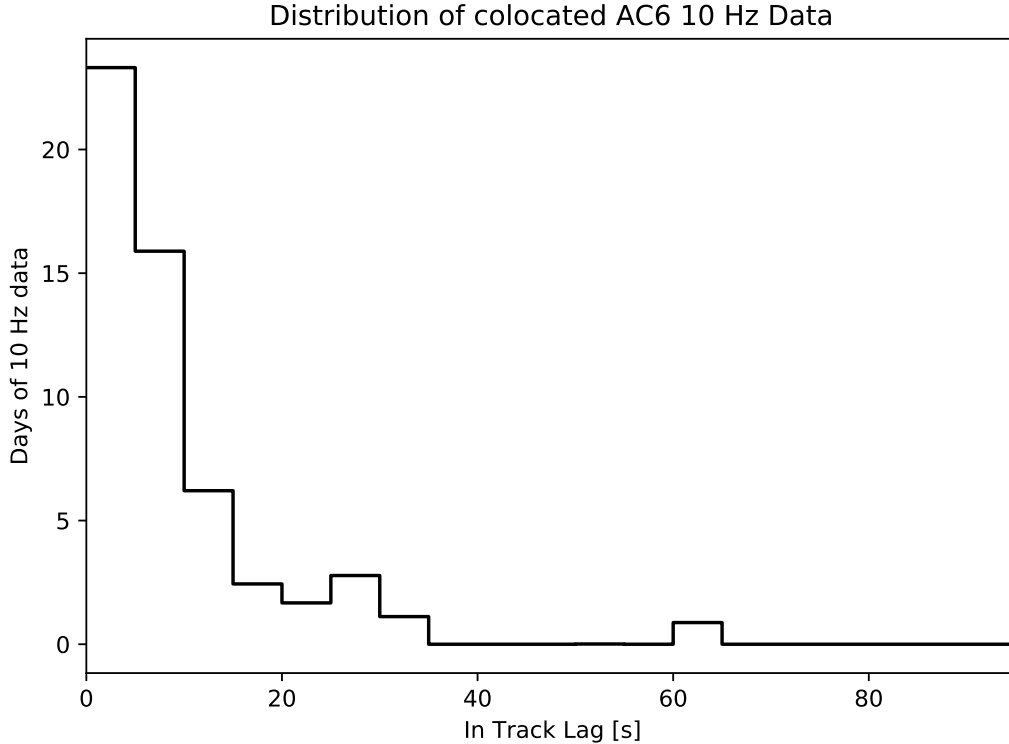


Figure A1. The distribution of colocated 10 Hz data as a function of in-track lag. Bins are 5 kilometers wide.

377 Appendix A Distribution of Colocated 10 Hz Data

378 Figure A1 shows the distribution of colocated AC6 10 Hz data as a function of in-
 379 track lag. This distribution is ~~weighted~~ *partially dominated by* small in-track lags and 72% of the colocated
 380 10 Hz data was taken when AC6 was separated in-track by less than 10 seconds, corre-
 381 sponding to 75 km in-track separation. Therefore, most of the curtains studied here were
 382 observed for small in-track lags.

, limits ability to explore upper end of Δt?

383 Acknowledgments

384 This work was made possible with the help from the many engineers and scientists at
 385 The Aerospace Corporation who designed, built, and operated AC6. M. Shumko was sup-
 386 ported by NASA Headquarters under the NASA Earth and Space Science Fellowship Pro-
 387 gram - Grant 80NSSC18K1204 and NASA Postdoctoral Program at the NASA's God-
 388 dard Space Flight Center, administered by Universities Space Research Association under
 389 contract with NASA. D.L. Turner is thankful for support from the Van Allen Probes
 390 mission and a NASA grant (Prime award number: 80NSSC19K0280). The work at The
 391 Aerospace Corporation was supported in part by RBSP-ECT funding provided by JHU/APL
 392 contract 967399 under NASA's Prime contract NAS501072. The AC6 data is available
 393 at <http://rbspgway.jhuapl.edu/ac6> and the IRBEM-Lib version used for this analysis can
 394 be downloaded from <https://sourceforge.net/p/irbem/code/616/tree/>.

395 References

- 396 Anderson, K. A., & Milton, D. W. (1964). Balloon observations of X rays in the

- auroral zone: 3. High time resolution studies. *Journal of Geophysical Research*, 69(21), 4457–4479. Retrieved from <http://dx.doi.org/10.1029/JZ069i021p04457> doi: 10.1029/JZ069i021p04457
- Blake, J. B., & O'Brien, T. P. (2016). Observations of small-scale latitudinal structure in energetic electron precipitation. *Journal of Geophysical Research: Space Physics*, 121(4), 3031–3035. Retrieved from <http://dx.doi.org/10.1002/2015JA021815> (2015JA021815) doi: 10.1002/2015JA021815
- Blum, L., Li, X., & Denton, M. (2015). Rapid MeV electron precipitation as observed by SAMPEX/HILT during high-speed stream-driven storms. *Journal of Geophysical Research: Space Physics*, 120(5), 3783–3794. Retrieved from <http://dx.doi.org/10.1002/2014JA020633> (2014JA020633) doi: 10.1002/2014JA020633
- Boscher, D., Bourdarie, S., O'Brien, P., Guild, T., & Shumko, M. (2012). *Irbem-lib library*.
- Breneman, A., Crew, A., Sample, J., Klumpar, D., Johnson, A., Agapitov, O., ... others (2017). Observations directly linking relativistic electron microbursts to whistler mode chorus: Van allen probes and FIREBIRD II. *Geophysical Research Letters*.
- Brown, R., Barcus, J., & Parsons, N. (1965, 6). Balloon observations of auroral zone x rays in conjugate regions. 2. microbursts and pulsations. *Journal of Geophysical Research (U.S.)*, 70. doi: 10.1029/JZ070i011p02599
- Comess, M., Smith, D., Selesnick, R., Millan, R., & Sample, J. (2013). Duskside relativistic electron precipitation as measured by sampex: A statistical survey. *Journal of Geophysical Research: Space Physics*, 118(8), 5050-5058. Retrieved from <https://agupubs.onlinelibrary.wiley.com/doi/abs/10.1002/jgra.50481> doi: 10.1002/jgra.50481
- Dietrich, S., Rodger, C. J., Clilverd, M. A., Bortnik, J., & Raita, T. (2010). Relativistic microburst storm characteristics: Combined satellite and ground-based observations. *Journal of Geophysical Research: Space Physics*, 115(A12).
- Douma, E., Rodger, C., Blum, L., O'Brien, T., Clilverd, M., & Blake, J. (2019). Characteristics of relativistic microburst intensity from sampex observations. *Journal of Geophysical Research: Space Physics*.
- Douma, E., Rodger, C. J., Blum, L. W., & Clilverd, M. A. (2017). Occurrence characteristics of relativistic electron microbursts from SAMPEX observations. *Journal of Geophysical Research: Space Physics*, 122(8), 8096–8107. Retrieved from <http://dx.doi.org/10.1002/2017JA024067> (2017JA024067) doi: 10.1002/2017JA024067
- Greeley, A., Kanekal, S., Baker, D., Klecker, B., & Schiller, Q. (2019). Quantifying the contribution of microbursts to global electron loss in the radiation belts. *Journal of Geophysical Research: Space Physics*.
- Johnson, A., Shumko, M., Griffith, B., Klumpar, D., Sample, J., Springer, L., ... others (2020). The firebird-ii cubesat mission: Focused investigations of relativistic electron burst intensity, range, and dynamics. *Review of Scientific Instruments*, 91(3), 034503.
- Lehtinen, N. G., Inan, U. S., & Bell, T. F. (2000). Trapped energetic electron curtains produced by thunderstorm driven relativistic runaway electrons. *Geophysical research letters*, 27(8), 1095–1098.
- Lorentzen, K. R., Blake, J. B., Inan, U. S., & Bortnik, J. (2001). Observations of relativistic electron microbursts in association with VLF chorus. *Journal of Geophysical Research: Space Physics*, 106(A4), 6017–6027. Retrieved from <http://dx.doi.org/10.1029/2000JA003018> doi: 10.1029/2000JA003018
- Lorentzen, K. R., Looper, M. D., & Blake, J. B. (2001). Relativistic electron microbursts during the GEM storms. *Geophysical Research Letters*, 28(13), 2573–2576. Retrieved from <http://dx.doi.org/10.1029/2001GL012926> doi: 10.1029/2001GL012926

- O'Brien, T. P., Blake, J. B., & W., G. J. (2016, May). *AeroCube-6 dosimeter data README* (Tech. Rep. No. TOR-2016-01155). The Aerospace Corporation.
- O'Brien, T. P., Looper, M. D., & Blake, J. B. (2019, July). *AeroCube-6 dosimeter equivalent energy thresholds and flux conversion factors* (Tech. Rep. No. TOR-2017-02598). The Aerospace Corporation.
- O'Brien, T. P., Lorentzen, K. R., Mann, I. R., Meredith, N. P., Blake, J. B., Fen nell, J. F., ... Anderson, R. R. (2003). Energization of relativistic electrons in the presence of ULF power and MeV microbursts: Evidence for dual ULF and VLF acceleration. *Journal of Geophysical Research: Space Physics*, 108(A8). Retrieved from <http://dx.doi.org/10.1029/2002JA009784> doi: 10.1029/2002JA009784
- Olson, W. P., & Pfitzer, K. A. (1982). A dynamic model of the magnetospheric magnetic and electric fields for july 29, 1977. *Journal of Geophysical Research: Space Physics*, 87(A8), 5943–5948. Retrieved from <http://dx.doi.org/10.1029/JA087iA08p05943> doi: 10.1029/JA087iA08p05943
- Parks, G. K. (1967). Spatial characteristics of auroral-zone X-ray microbursts. *Journal of Geophysical Research*, 72(1), 215–226.
- Partamies, N., Donovan, E., & Knudsen, D. (2008). Statistical study of inverted-v structures in fast data. In *Annales geophysicae* (Vol. 26, pp. 1439–1449).
- Randall, C. E., Harvey, V. L., Holt, L. A., Marsh, D. R., Kinnison, D., Funke, B., & Bernath, P. F. (2015). Simulation of energetic particle precipitation effects during the 2003–2004 arctic winter. *Journal of Geophysical Research: Space Physics*, 120(6), 5035–5048.
- Seppälä, A., Douma, E., Rodger, C., Verronen, P., Clilverd, M. A., & Bortnik, J. (2018). Relativistic electron microburst events: Modeling the atmospheric impact. *Geophysical Research Letters*, 45(2), 1141–1147.
- Shumko, M., Johnson, A., Sample, J., Griffith, B. A., Turner, D. L., O'Brien, T. P., ... Claudepierre, S. G. (2019). Electron microburst size distribution derived with aerocube-6. *Journal of Geophysical Research: Space Physics*, e2019JA027651.
- Thorne, R. M., O'Brien, T. P., Shprits, Y. Y., Summers, D., & Horne, R. B. (2005). Timescale for MeV electron microburst loss during geomagnetic storms. *Journal of Geophysical Research: Space Physics*, 110(A9). Retrieved from <http://dx.doi.org/10.1029/2004JA010882> (A09202) doi: 10.1029/2004JA010882
- Tsyganenko, N. (1989). A solution of the chapman-ferraro problem for an el lipsoidal magnetopause. *Planetary and Space Science*, 37(9), 1037 - 1046. Retrieved from <http://www.sciencedirect.com/science/article/pii/0032063389900767> doi: [http://dx.doi.org/10.1016/0032-0633\(89\)90076-7](http://dx.doi.org/10.1016/0032-0633(89)90076-7)